INTERNATIONAL JOURNAL OF
NUMERICAL ANALYSIS AND MODELING
Volume 9, Number 3, Pages 628–643

COUPLED FLOW– AND ROCK MECHANICS SIMULATION: OPTIMIZING THE COUPLING TERM FOR FASTER AND ACCURATE COMPUTATION

ØYSTEIN PETTERSEN

Abstract. Coupled flow and rock mechanics simulations are necessary to achieve sufficient understanding and reliable production forecasts in many reservoirs, especially those containing weak or moderate strength rock. Unfortunately these runs are in general significantly more demanding with respect to computing times than stand-alone flow simulations. A scheme is presented whereby the number of needed rock mechanics simulations in such a setting can be reduced to a minimum. The scheme is based on constructing optimal input for flow simulations from a few rock mechanics runs. Results obtained with the scheme are at least as accurate as traditional coupled runs, but computations are considerably faster, often as much as two orders of magnitude.

Key Words. Reservoir simulation, Coupled simulation, Rock mechanics, Compaction

1. Introduction

Production forecasts in petroleum reservoirs are most often computed by reservoir simulators, based on numerical solution of the equations for flow in porous media. In most or many reservoirs the compaction of the porous rock will have strong influence on pressure development and flow pattern, and as such is an important parameter to model reliably. In the flow equations, fluid pressure is the only present parameter that these compaction computations can be based on. In reality, however, compaction depends on reservoir rock behaviour, which may be nonlinear poro-elasto-plastic, depending on stress path, temperature, and possibly water content [8]. Hence it is widely accepted in the community that rock-mechanics simulations, preferably coupled flow– and rock mechanics simulations are necessary when accurate compaction computation is required, which is the case for most reservoirs, possibly excluding reservoirs comprised solely of strong or hard rock.

An example of results obtained by employing different strategies for compaction computation is shown in Figure 1, where simulated oil production and water cut (fraction of produced water to total liquid production) from a producing well in a fluvial reservoir is depicted for the three different cases, i) assuming permeability k does not change under compaction, ii) assuming k is a function of fluid pressure, $k = k(p_f)$, and iii) the correct formulation, k is a function of stress (in this case mean effective stress p'), $k = k(p')$.

From the figure it can be clearly seen that the choice of compaction model can have large consequences for e.g. production predictions. The stress distribution in the reservoir is dependent on properties in the surrounding rock as well as within

Received by the editors November 26, 2010 and, in revised form, August 1, 2011.
2000 *Mathematics Subject Classification.* 35R35, 49J40, 60G40.

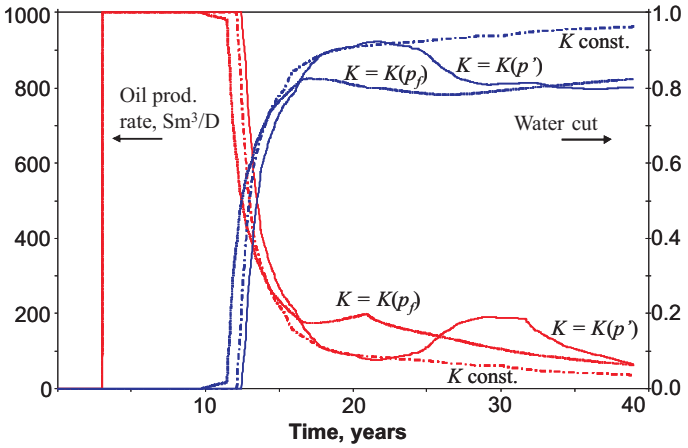

FIGURE 1. Oil and water production in one well; three different models for how permeability varies with load

the reservoir, and hence is distributed in a manner which cannot be caught by the pressure state alone. An example is shown in Figure 2, where (simulated) permeability multipliers (ratio of current to initial permeability) are shown in a reservoir cross section transverse to a system of initially high-permeability channels in a relatively strong background material. Figure 2a shows the multipliers when modelled as functions of fluid pressure, while Fig. 2b shows the more accurate distribution when modelled as a function of stress, and clearly shows how the channel compaction influences larger parts of the reservoir cross section (internal stress arching). In general the rock mechanics boundary conditions have large impact on the compaction distribution in the reservoir, which is a major reason that the compaction cannot be a function of the pressure only.

During the last few decades there has been a growing awareness that a complete understanding of reservoir dynamics frequently also requires understanding of the interaction between fluid flow and rock mechanics. One example is the change of porosity and permeability due to the deformation of reservoir rock, which is a consequence of the changing stress field within and surrounding the reservoir, and how these altered conditions influence the fluid flow in the porous medium. As the coupling between these mechanisms is strong the full coupled system (Eqns. 1–5 below) should ideally be solved simultaneously. The main reasons for seeking alternatives to such a scheme are, i) The simultaneous solving of the coupled system can be prohibitively expensive (in terms of computing time), and ii) Commercial flow simulators offer a rich set of options for reservoir management, and in the same manner commercial stress simulators offer a multitude of rock behaviour models. No existing fully coupled simulators include all the options that "specialist" users need and do not wish to sacrifice for the benefit of using a single simulator. Hence alternative coupling schemes have been sought. In order of increasing complexity these include, one-way coupling, one-way coupling with feedback, two-way coupling, and two-way coupling with pore volume iterations [3, 4, 5, 6, 7, 8, 9, 13, 14, 15, 17]. For a relatively complete description, see [11] and the references herein.

The focus in this paper is on the coupling mechanism, and especially how the coupling term can be modified to achieve fast and accurate solutions. The coupling term was discussed by e.g. Gutierrez [4], Dean et *al.* [2], and Mainguy and

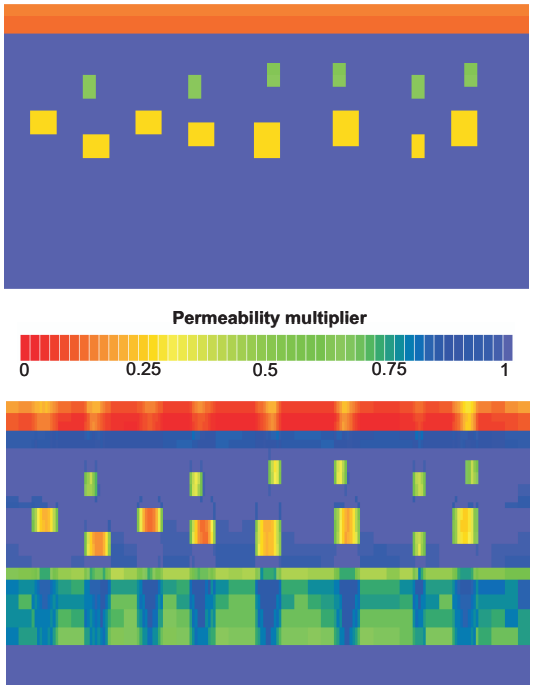

FIGURE 2. Permeability multipliers in a reservoir cross section. a) (top) Assuming k function of pressure. b) (bottom) k function of stress

Longuemare [9]. In the latter paper it was noted that the term was not important in coupled simulation, as the correct compaction would be computed by the process anyway. While this remark is true, it does not take computing time into account, as the required work to compute the term if the initial guess is far off will be considerable. Hence, in this paper we construct a coupling term such that computing time will be significantly reduced without loss of accuracy. In later sections, the relevance of the coupling term, and how it enters the different coupling modi will be discussed.

In previous papers we have presented the procedure and results obtained on studies on idealized Valhall and Gullfaks segment models [11, 12]. In this paper we establish a theoretical foundation for the method, and validate the scheme.

2. Model Formulation

As the main interest is on the coupling mechanism between fluid flow and rock behaviour, the individual model equations or numerical schemes do not need to, and will not be analysed. For completeness the equations are presented below. The analysis of the coupling is not dependent on how these equations are formulated, hence for convenience a simplified case is shown; for flow of oil (o) and water (w) in an isotropic porous rock, under isothermal conditions and neglecting capillary pressure.

Fluid Flow Equations.
(Two-phase black oil formulation):

$$\begin{aligned} &\nabla \cdot \left\{ \tfrac{k k_{rl}}{\mu_l} (\nabla p_f - \gamma_l \nabla z) \right\} = \tfrac{\partial}{\partial t} \left(\tfrac{\phi S_l}{B_l} \right) + q_l, \quad l = o, w \\ &S_o + S_w = 1 \end{aligned} \tag{1}$$

The parameters entering these equations are, permeability (conductivity) k, relative permeability $k_{rl} = k_{rl}(S_w)$, fluid pressure p_f, the gravity term γ_l, porosity ϕ, fluid saturations S_l, the fluid volume factors B_l (ratio of reference volumes measured at reservoir and surface conditions), and the source terms q_l.

Also of interest in this context is the standard flow simulator model for rock compaction:

$$\phi = \phi(p_f) \text{ and } k = k(p_f) \tag{2}$$

Rock Mechanics Equations.
Elastoplastic stress–strain relationship:

$$\delta\sigma_{ij} = \sum_{k,l} D_{ijkl}(\varepsilon_{kl} - \varepsilon^p_{kl}) - \Delta p_f \delta_{ij} \tag{3}$$

$\boldsymbol{\sigma}$ and $\boldsymbol{\varepsilon}$ are the stress and strain tensors, and $\boldsymbol{D}$ is the matrix of elastic constants. δ_{ij} is the Kronecker delta, being unity when $i = j$, zero else. Superscript p is used to denote the plastic part of the deformation.

Eq. 3 expresses the material deformation as strain response to applied stress. In absence of the inelastic term $\boldsymbol{\varepsilon}^p$, the equation is reduced to the standard linear stress–strain relationship as stated in one dimension by the well-known Hooke's law

$$\varepsilon = \frac{1}{E}\sigma,$$

where E is Young's modulus.

At this point it should be noted that numerical solutions to pure elasticity problems are relatively easily computed, and the aforementioned issue of unacceptable computing times typically does not apply to elastic materials. Unfortunately very few reservoir rocks or soils behave elastic [10, 12], and more general and complex models for material behaviour and failure are needed.

The description can be illustrated by the behaviour of granular materials like sand. In response to an applied external stress a soil volume will be compressed, but as the grain compressibility is negligible compared to total compressibility, the volume change will be completely taken up by pore volume reduction, by reorganization of the grains [10]. Each level of applied stress corresponds to a stable grain packing, which is a characteristic of the material and the stress level. As the grains become tighter packed, further packing becomes increasingly harder to achieve – material hardening. On the other hand, relieving stress will not change the packing noticeably, as that would alter the packing state to a less stable one, contradicting the physical principle of nature seeking the most stable states. Hence in contrast to the elastic case the material properties are continuously changing during compression, or alternatively formulated, each compression level defines a "new" material characterised by current packing.

In the general formulation the deformation or failure characteristics of a material is described in the stress space $(\sigma_1, \sigma_2, \sigma_3)$, where $\sigma_1, \sigma_2, \sigma_3$ are the principal stresses. In this space the *yield surface* is a closed surface $g(\sigma_1, \sigma_2, \sigma_3) = 0$ such that for any stress state interior to the yield surface the material behaves elastically. Stress states outside the surface are unattainable, and if a state is attempted

changed such that the resulting state would be outside the yield surface, the new stress state can only be reached by expanding the yield surface – corresponding to permanent deformation or failure of the material. Comparing to the grain pack model the increasingly tighter grain packing by increasing load corresponds to expansion of the yield surface, while unloading or reloading correspond to stress states which reside entirely within the current yield surface. The loading process which corresponds to expansion of the yield surface is denoted *primary loading*, while loading and unloading at levels below the hitherto largest load are denoted secondary loading/unloading.

A multitude of failure models have been developed; describing the shape and expansion of the yield surface as a response to stress change, and how the material characteristics (including failure) change as a function of the dynamic yield surface.

In the general case the expansion of the yield surface is described by an equation of the form; (For simplicity the special case where where the yield surface coincides with the plastic potential surface is shown.)
Yield surface expansion (plastic flow rule):

$$\delta\varepsilon_{ij}^{p} = \delta\lambda\frac{\partial g}{\partial\sigma_{ij}} \tag{4}$$

where λ is a plastic multiplier and the yield surface is defined by $g = 0$.

The changing of material properties ("hardening" or "softening") is described by the hardening rule:

$$dg(\chi) = 0 \tag{5}$$

where χ is the "hardening parameter", determining the rate of expansion of the yield surface.

The different failure models also define $g(\sigma_1, \sigma_2, \sigma_3)$ in closed form. For examples see e.g. [10, 18].

Solving Eqns. 4–5 in a numerical scheme can be very demanding, and the main reason why stress simulations including plastic material deformations often requires much computing time.

Lastly it should be noted that the principal stresses are not always the most convenient parameters to use in combination with a fixed physical space. The basis for the stress space is therefore commonly defined by *stress invariants* $\mathbf{J} = (J_1, J_2, J_3)$, so that the yield surface becomes $g(\mathbf{J}, \chi) = 0$.

A frequently used set of stress invariants is;

$$\begin{aligned}
\text{Mean stress:} \quad & J_1 = p && = \frac{1}{3}(\sigma_1 + \sigma_2 + \sigma_3) \\
\text{Deviatoric stress:} \quad & J_2 = \tfrac{q}{\sqrt{3}} && = \sqrt{\frac{(\sigma_1 - \sigma_2)^2 + (\sigma_2 - \sigma_3)^2 + (\sigma_3 - \sigma_1)^2}{6}} \\
\text{Lode's angle:} \quad & J_3 = \theta && = \tan^{-1}\left[\frac{1}{\sqrt{3}}\left(2\frac{(\sigma_2 - \sigma_3)}{(\sigma_1 - \sigma_3)}\right) - 1\right] \quad -30^\circ \le \theta \le 30^\circ
\end{aligned}$$

where $(\sigma_1, \sigma_2, \sigma_3)$ are principal stresses.

In a coupled solution of flow in a porous medium, the effective (current) porosity and permeability are functions of the stress state as computed by Eqns. 3–5. The pore pressure as computed by Eq. 1 is directly related to the porosity, while the permeability has strong influence on flow velocity and saturations. On the other hand, the stress calculations are dependent on the pore pressure through Eq. 3. Hence stress and pore pressure have mutual influence, which signifies that the system 1–5 must be solved implicitly.

3. The Coupling Term

The flow equations 1 and the rock mechanics equations 3–5 are coupled primarily by the volumetric change of the porous rock (compaction or expansion). The volumetric change is directly related to the strain $\boldsymbol{\varepsilon}$, and influences the flow equations through the porosity ϕ and permeability k. Especially for weak rocks the volumetric change can have great impact on these two parameters. E.g. observations from several North Sea reservoirs show a permeability reduction of 20–90% at a load increase of 100 bars [12]. Hence the coupling between the flow equations and rock mechanics equations is generally relatively strong.

When the flow equations are solved as a stand-alone problem, it is normally assumed that rock compressibility is a function of pressure:

$$c_r^F(p_f) = -\frac{1}{V}\frac{\partial V}{\partial p_f}$$

(Rock compressibility is denoted by c_r, with superscript F used when the compressibility was computed by the flow equations, and superscript R when derived from the rock mechanics.)

This is a natural approach, as rock compressibility in most cases is too important to neglect, and p_f is the only available parameter for calculating compaction in the flow equations. In a porous rock, especially in granular materials as sand or sandstone, the compressibility is dominated by the behaviour of the pore space, not the solid (grains) [10]. The net force acting on the pore walls and governing the compression of the pore space, is the difference between the external total stress and the internal fluid pressure. It is thereby appropriate to model compaction in a porous rock as a function of the *effective stress* $\boldsymbol{\sigma}'$:

$$\boldsymbol{\sigma}' = \boldsymbol{\sigma} - \boldsymbol{I}\alpha p_f \tag{6}$$

Here $\boldsymbol{I}$ is the identity tensor and α Biot's constant. When the solid is incompressible, $\alpha = 1$, which we assume for convenience, without loss of generality.

For compaction calculations we adopt the commonly used model that pore volume change is a function of the *mean effective stress* p'. Eq. 6 can then be written as:

$$p' = p - p_f \tag{7}$$

where $p = \mathrm{tr}(\boldsymbol{\sigma})/\boldsymbol{3}$ (tr() is the sum of the tensor diagonal terms), and $p' = \mathrm{tr}(\boldsymbol{\sigma}')/3$.

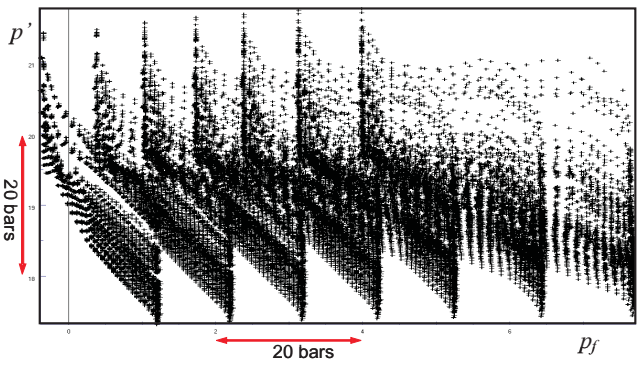

FIGURE 3. Correlation: Mean Effective Stress vs. Fluid Pressure

From Eq. 7 we see that the assumption of pressure-dependent compaction used when solving the stand-alone flow problem is only valid if p_f is a function of p', which is very seldom the case.

In Figure 3, which is taken from a simulation study on a Valhall segment, cell values of p' vs. p_f have been plotted for all cells in the mesh at several time steps. The figure clearly shows that any value of the fluid pressure corresponds to a number of mean effective stressvalues, hence invalidating the "compaction vs. fluid pressure" concept. As a consequence, we reiterate that coupled flow– and rock mechanics simulations are necessary if accurate compaction computation is needed. Hence, as the rock mechanics simulations cannot be avoided, the goal is to minimize the number of these often costly runs (in terms of computing time).

In the following a procedure will be derived and described, where an optimal coupling term is constructed from only a few rock mechanics simulations. Using this coupling term makes it possible to often do further studies by stand-alone flow simulations, or if rock simulations are needed, the number of additional such runs will be reduced to a minimum. (In many studies the results from the rock mechanics simulations are at least as important as the flow simulation part, and in such cases there is obviously no desire to eliminate these runs.)

Define a function m, the *pore volume multiplier*, $m = PV/PV_0$, where PV is pore volume and subscript 0 denotes initial. (In a simulation context, PV would typically be taken as cell values, while in general we could use some REV (representative elementary volume) or unit reference volume.) m is used in preference to porosity, but plays the same role. m is a function of load, normally non-increasing with load and equal to unity at no-load. In a flow simulation context m is required to be a non-decreasing function of pressure. (Note that in a producing reservoir increasing load corresponds to pressure reduction.)

The traditional flow simulator compaction model is then based on the assumption $m = m(p_f)$ and similar for permeability, $k = k(p_f)$, ref. Eq. 2.

Based on the observations above, the relationship should be, $m_\sigma = m_\sigma(p', \boldsymbol{x})$ and $k = k(p', \boldsymbol{x})$, where the subscript σ has been introduced to accentuate the dependency on stress.

Note that as both m and k are non-increasing functions of p' a relation between them exists: $k = k(m)$. We will therefore not discuss k in the following, but assume that it can be derived from m when needed.

For the following discussion the detail description, Eqns. 1–5 are not needed. We therefore rewrite the system in simplified form:

$$\text{Flow equations:} \quad \boldsymbol{F}(\boldsymbol{x}, p_f, S_w) = \boldsymbol{0} \tag{8}$$

$$\text{Rock mech. equations:} \quad \boldsymbol{R}(\boldsymbol{x}, \boldsymbol{\varepsilon}, \boldsymbol{\sigma}, \boldsymbol{u}) = \boldsymbol{0} \tag{9}$$

In these equations the dependencies between the state variables are,

$$\begin{aligned}
p_f &= p_f(m; \boldsymbol{x}) \\
S_w &= S_w(k; \boldsymbol{x}) \\
k &= k(p'; \boldsymbol{x}) \\
\boldsymbol{\varepsilon} &= \boldsymbol{\varepsilon}(\boldsymbol{u}) = \boldsymbol{\varepsilon}(\boldsymbol{\sigma'}, p_f; \boldsymbol{x}) \\
\boldsymbol{u} &= \boldsymbol{u}(\boldsymbol{\sigma'}, p_f; \boldsymbol{x}) \\
\boldsymbol{\sigma} &= \boldsymbol{\sigma}(\boldsymbol{x}) \\
m &= m(p'; \boldsymbol{x}) \\
p' &= p - p_f
\end{aligned}$$

(Time dependency has been suppressed.)

In a pragmatic sense we can regard pore pressures and saturations as the output from a black box reservoir simulator, and stress, strain and deformations (by the displacement vector $\boldsymbol{u}$) as the output from a black box stress simulator. The coupling between the simulators is defined by the mean effective stress p' and the pore volume multiplier m, and can be handled externally to the simulators.

The coupling scheme presented in this paper is not dependent on the specific simulators or numerical schemes used. We have used three different commercial finite element stress simulators and two different finite difference reservoir simulators. For simplicity of data exchange (avoiding interpolation) identical grids were always used in the finite element and finite difference meshes (although higher order finite elements were allowed).

Calculation of pore volume multipliers from stress or strain is obviously a critical part of the coupling. Various formulations have been proposed in the literature, e.g. [15, 18]. The following was suggested by Chin and Thomas [1] and Sylte et *al.* [16], based on the *volumetric strain* $\varepsilon_V = \mathrm{tr}(\boldsymbol{\varepsilon})$, and is widely used (e.g. on the Valhall field):

During compression the porosity is changed due to reorganization of the solid structure (grains). In addition, the reference bulk volume is altered by volumetric compaction:

$$\begin{array}{ll} \text{New effective porosity:} & \phi = 1 - (1-\phi_0)e^{\Delta\varepsilon_V} \\ \text{Updated PV-multiplier:} & m = \frac{e}{e_0} = \frac{\phi/(1-\phi)}{\phi_0/(1-\phi_0)} \end{array} \tag{10}$$

(e is voids volume, and subscript 0 denotes initial value.)

4. Solving the Coupled System

Ideally the full system 8–9 should be solved at each time step. As noted above, and also as a consequence of the arguments below a fully implicit scheme is needed.

Assume the system 8–9 is solved by a staggered scheme, i.e. from the solution at time t, first $\boldsymbol{F}^{t+\Delta t}(\cdot) = \boldsymbol{0}$ is solved. Then the fluid pressure $p_f(\boldsymbol{x}, t+\Delta t)$ is used to initialize effective stress when solving $\boldsymbol{R}^{t+\Delta t}(\cdot) = \boldsymbol{0}$. As the fluid pressure is required to solve $\boldsymbol{R}^{t+\Delta t}(\cdot) = \boldsymbol{0}$, $\boldsymbol{F}^{t+\Delta t}(\cdot) = \boldsymbol{0}$ must be solved first in the sequence. The computed $p_f(\boldsymbol{x}, t+\Delta t)$ is strongly dependent on the m-function used in the flow equations, but this m-function is not known before the rock mechanics equations have been solved, and hence must be estimated at first use. Schematically, the solving procedure can be defined as, i) The system $\boldsymbol{F}^{t+\Delta t}(\cdot) = \boldsymbol{0}$ is solved using the estimated $m^0(p_f, \boldsymbol{x})$. The outcome is cell values of fluid pressure and compaction: $\{p_f, c_r^F\}_i$, with i running over all cells. ii) The rock mechanics equations are initialized with effective stress defined by the fluid pressure state found in i). The system $\boldsymbol{R}^{t+\Delta t}(\cdot) = \boldsymbol{0}$ is solved. From the resulting state the strain-derived compaction is computed (Eq. 10): $c_r^R(\boldsymbol{x_i}, t+\Delta t)$. iii) If $\|c_r^F - c_r^R\| < \varepsilon_{tol}$ convergence has been achieved. Else compute the adjustment ratio,

$$r_c(\boldsymbol{x}_i) = \frac{c_r^R(\boldsymbol{x}_i, t+\Delta t)}{c_r^F(\boldsymbol{x}_i, t+\Delta t)}$$

and update all cell pore volumes at time t by multiplying the present values with $r_c(\boldsymbol{x}_i)$. Repeat procedure from i), using the updated pore volumes.

Evidently, when cell pore volumes are updated in this manner, the cell fluid pressures will also change, and thereby the revised pore volumes are still not consistent with the pressure state. Although the procedure is guaranteed to converge [15],

the total computing time can be, and normally is considerable. (Solving the rock mechanics equations often requires at least an order of magnitude more than the flow equations.) The drawback with this iterative procedure is that when the pore volumes are updated as described the reservoir description itself is changed at discrete times, hence also changing the dynamics of the system. Moreover, the error introduced by using the "wrong" compaction function will propagate with time, irrespective of the size of Δt. Hence an explicit scheme, even with pore volume update will not be able to compute accurate compaction.

An alternative approach which we will pursue would be, in place of changing the reservoir description, to find a better initial estimate of $m(p_f)$ such that when this m-function is used in the flow equations the computed c_r^F will agree with c_r^R , hence confirming their values, such that no further iterations will be needed.

Due to the computer-time needed to solve the rock mechanics equations, the system $\boldsymbol{R}(\cdot) = \mathbf{0}$ in many implementations is not solved at every time step, but only at selected times, denoted *stress steps*. The gain is obviously that the rock mechanics equations will be solved fewer times during a coupled simulation, but on the other hand the ratio r_c will probably drift away from unity when Δt is increased, so that more pore volume iterations will be required for convergence.

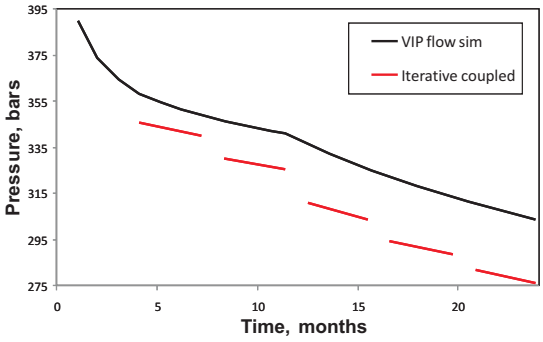

FIGURE 4. Discontinuous pressure development as computed by iterative coupled simulation

A disadvantage of only solving the rock mechanics equations at the stress steps is that the solution of the full system, including pressure and compaction, will only be accurate at the stress steps themselves, and follow the erroneous trend from the m-function estimate between stress steps. This "feature" has been observed in practice and is shown in Figure 4. The stress steps can be identified by the discontinuities in the red line. At the start of each stress step, pore volumes and fluid pressures are correct, but the trend between the stress steps is a result of the (erroneous) m-function estimate.

5. Principles of Construction Procedure

The goal is to construct an alternative function $m(p_f)$ for use when solving the flow equations, such that the compaction and pressure state is accurate already at the flow equation stage. By the discussion above, the cell compaction c_r^R found by $\boldsymbol{R}(\cdot) = \mathbf{0}$ will then equal c_r^F in all cells. In practice it may not be even theoretically possible to find such an m-function. In that case we seek the best approximation and can be assured that it will be the optimal initializer for the rock mechanics system.

In the effective stress $p' = p - p_f$, the total mean stress $p(\boldsymbol{x}, t)$ in a primary loading process is primarily governed by external forces, which do not change much during reservoir depletion. $p(\boldsymbol{x}, t)$ can have, and often has, large spatial variation, but for fixed $\boldsymbol{x}$ the dependency on time and fluid pressure variation is weak. The effective stress is on the other hand primarily tied to pore collapse and grain reorganization, especially in weak materials as sand or sandstone [10]. p' will therefore typically respond rapidly to changes in fluid pressure, both in time and space. Hence we can expect,

$$\left.\frac{\partial p}{\partial p_f}\right|_x \ll \left.\frac{\partial p'}{\partial p_f}\right|_x \tag{11}$$

We split the effective stress into two terms,

$$p'(p_f, p; \boldsymbol{x}) = p'_p(p_f; \boldsymbol{x}) + \tilde{p'}(p_f, p; \boldsymbol{x}) \tag{12}$$

where p'_p is the projection of p' on the p_f-space.

Using Eq. 11 then

$$p'(p_f, p; \boldsymbol{x}) \approx p'_p(p_f; \boldsymbol{x}) \tag{13}$$

Hence:

> In a primary loading process, *locally* (for fixed $\boldsymbol{x}$), mean effective stress is approximately a function of fluid pressure alone.

Note: The relation 13 can only be expected to be valid during primary loading (depletion). During unloading or reloading, the pore volume change in response to stress changes can be very different, except if the material is in the elastic domain. As an example the pore volume in weak materials will often remain constant during unloading [10].

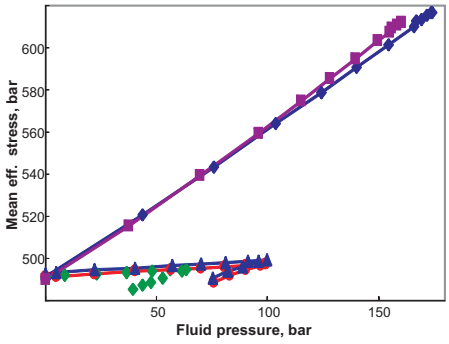

FIGURE 5. p' vs. p_f for fixed $\boldsymbol{x}$ (cell), for some cells

The statement above has been validated by numerical experiments: the relationship between p' and p_f in a single cell was recorded for all cells, in a number of different simulation studies. The results were consistently in agreement with Eq. 13. A few representative examples are shown in Fig. 5, taken from a study on a Valhall segment. (The irregular points in the lower curves are from unloading–reloading, and should be disregarded in this context, in agreement with the comment above.)

Next, observe that the total energy in the system is primarily determined by the flow equations – energy is added and removed by production / injection wells, and fluid and rock volume changes, mechanisms which are taken care of by the flow equations. The rock mechanics equations will distribute the compression energy

according to $\boldsymbol{R}(\cdot) = \mathbf{0}$, essentially conserving the total energy. The significance of this is that if two cases have identical material properties and boundary conditions, and differ only by the total initialisation energy, the stress *magnitudes* will be different, but the qualitative stress-distribution will be equal in the two cases.

Based on the observations above, we state that m-functions can be defined as: Locally (for fixed $\boldsymbol{x}_i$):

$$m(p_f, p; \boldsymbol{x}_i) = m_p(p_f; \boldsymbol{x}_i) + \tilde{m}(p_f, p; \boldsymbol{x}_i) \tag{14}$$

where m_p is the projection of m on the p_f-space. During primary loading,

$$m(p_f, p; \boldsymbol{x}_i) \approx m_p(p_f; \boldsymbol{x}_i) \tag{15}$$

Hence, when attempting to construct an optimal m-function, according to Eq. 15, the m-function can be defined as a function of pressure, but a separate relationship will be needed in every cell.

6. Construction Process

First the flow equations $\boldsymbol{F}(\cdot) = \mathbf{0}$ are solved at time t_1, using an estimated m-function $m^0(p_f, \boldsymbol{x}_i)$. The resulting fluid pressure and corresponding compaction in cell $\boldsymbol{x}_i$ is $p_f(\boldsymbol{x}_i)$ and $c_r^F(\boldsymbol{x}_i) = m^0(p_f(\boldsymbol{x}_i))$, while the correct values would be some (p_{fi}^*, c_{ri}^{F*}), which are unknown, as the actual compaction relationship is still not known. The function m_p (Eq. 15) is the unique relationship for compaction vs. fluid pressure in cell $\boldsymbol{x}_i$. Obviously, the point (p_{fi}^*, c_{ri}^{F*}) must lie on the curve $m = m_p(p_f, \boldsymbol{x}_i)$.

Next, the rock mechanics system $\boldsymbol{R}(\cdot) = \mathbf{0}$ is solved at time t_1, using the pressure state $\{p_f(\boldsymbol{x}_i); i = 1, \ldots, N_{mesh}\}$ as initializer. Using the cell volumetric strain values $\varepsilon_V(\boldsymbol{x}_i)$ from this solution the rock mechanics cell compaction $c_r^R(\boldsymbol{x}_i) = m_\sigma(\varepsilon_V, \boldsymbol{x}_i)$ is computed from Eq. 10. As noted above; as the initialisation pressure was a function of the (probably erroneous) estimate m^0, the calculated value $c_r^R(\boldsymbol{x}_i)$ is also generally incorrect. However, the key observation now is that the computed point $[p_f(\boldsymbol{x}_i), c_r^R(\boldsymbol{x}_i)]$ must lie on the curve $m = m_p(p_f, \boldsymbol{x}_i)$ introduced above. This is because the stress state computed by $\boldsymbol{R}(\cdot) = \mathbf{0}$ with the applied initial and boundary conditions is a *permitted solution* to the problem with material properties and loads as defined. Varying the cell pressures in a manner that is consistent with the flow equations implies varying the total compaction energy in the reservoir, and as long as the materials and the load process remains the same, all realisations are possible reservoir states with the applied constraints. Independent of the choice of $m^0(p_f, \boldsymbol{x}_i)$, all such points $[p_f(\boldsymbol{x}_i), c_r^R(\boldsymbol{x}_i)]$ will lie on the same curve.

To generate additional points on the curve $m = m_p(p_f, \boldsymbol{x}_i)$ the procedure is repeated for other load values, i.e. in practice by different pressure values. The easiest and most consistent way to achieve this is to solve the coupled system, Eqns. 8–9, at several time steps $t_1, t_2, t_3, \ldots$ in a depletion process, i.e. such that the average fluid pressure is steadily decreasing. How many such solutions are needed to construct the m_p-function obviously depends on the complexity of the variation of m with p_f. In practice we have found that about 6 solutions of the coupled system normally suffices.

Care must be taken to use only points from primary compaction. As noted, except for cases when the rock behaves elastically, unloading and reloading will be along different curves from the primary loading curve (the two lower curves in Fig. 5). As a consequence, the m-curves should be constructed from primary load data, and only used during primary load when solving the flow equations. Unloading and reloading should be handled by appropriate hysteresis branches on the m-curves.

6.1. Practical Considerations.

In principle the m-curves could be used as constructed, with one curve for each grid cell, as most commercial flow simulators allow for this (although for meshes with more than about one million cells computer memory would become a limitation). It is, however, convenient to reduce the number of curves. Hence we have chosen to merge m-curves which differ less than a pre-defined error tolerance.

Apparently the success of the described procedure depends on the validity of Eq. 15. If this equation was exact, the generated m-curves would be perfect, and no further rock mechanics simulations would be needed. In practice evidently Eq. 15 is only approximately valid. The reservoir stress state will to a large extent be dependent on boundary conditions, both at external boundaries and at internal boundaries separating materials with different properties. This boundary dependency will be well taken care of by the splitting shown in Eq. 15, which implies that a significant part of the qualitative rock state will be adequately handled by the described approach. On the other hand, many physical situations in rock mechanics exist which are impossible to approximate with a simplified procedure as described. One example is dilation, where the rock expands locally with increasing mean stress. As flow simulators require the m-functions to be non-decreasing with pressure, dilation is not even theoretically possible to include in the m-curves. Also other local variations will probably be impossible to account for when assuming a splitting as in Eq. 15.

The way the m-functions were constructed, for each $\boldsymbol{x}_i$, $m = m_p(p_f, \boldsymbol{x}_i)$, being the projection, is the best possible approximation to the general $m(p_f, p; \boldsymbol{x}_i)$ in p_f-space. Hence it is the optimal pore volume multiplier to use when solving $\boldsymbol{F}(\cdot) = \boldsymbol{0}$. When Eq. 15 is uniformly a good approximation, the cell compaction will be accurate in all grid cells already by the flow equations. In the general case where the approximation is not sufficiently good (either locally in space or due to effects which cannot be captured), the constructed m-functions will still be the optimal initialiser for solving the rock mechanics system. In this case an additional coupled run must be performed as a corrector, but this run can be done at minimum cost (without iterations) compared to using the "standard" m-functions.

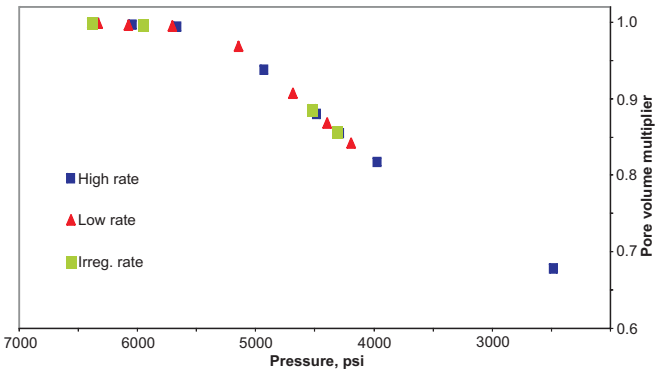

FIGURE 6. Points defining m-function, by three different construction processes

The constructed m-functions are independent of the production dynamics used during construction. The m-curves are directly dependent on the rock mechanical properties and boundary conditions, so if these are changed a reconstruction will

obviously be required. In general a reservoir is a closed system, except for injection or production wells. Well positions are part of the boundary conditions, and as such reconstruction is needed when well positions are changed. In practice we have however experienced that a set of m-functions work reasonably well also when used with altered well positions. On the other hand, well production– or injection rates have no impact on the curves, due to all computed states being permitted solutions to the configuration in question. This was tested by simulating the same setup with three different loading approaches, firstly with high depletion rate (where average reservoir pressure was rapidly decreasing), secondly with low rate, and lastly with irregular rate variation, combining pressure depletion and build-up at varying rates. The resulting points $[p_f(\boldsymbol{x}_i), m_\sigma(\boldsymbol{x}_i)]$ (in one cell) from these simulations are shown in Figure 6 – the same m-curve is obtained irrespective of the process by which it was constructed.

7. Results

Results from using the procedure in various reservoir production problems have been presented elsewhere [11, 12]. In this context some figures demonstrating the use and quality of the method itself are presented.

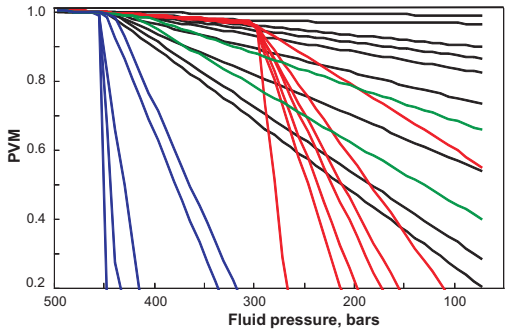

FIGURE 7. Excerpt of m-curves generated for a single material (from Valhall study) (colour coding only for clarity)

Figure 7 shows some of the m-curves that were generated for a single material, i.e. a rock that was represented with a single m-curve in the original flow simulation. The figure clearly demonstrates that it is not possible to account for the spatial variation of the compaction using the traditional flow simulation concept of one (and only one) curve for each rock type. The large difference between the generated curves can mostly be explained by boundary influence: The curves with the least variation are for cells near the reservoir boundary, while the largest variation is seen in areas where the boundary influence is weak or absent.

Figures 8 and 9 give an indication of the quality of the final simulations. Both figures show correlation between cell pore volume multipliers computed by the flow simulator m-function, and "exact" pore volume multipliers as computed by an iterative coupled simulation. In Fig. 8 the "standard" flow simulator m-function concept was used, while Fig. 9 shows the result of using the modified functions as described. The improvement is considerable.

Figure 10 is the companion to Fig. 4. When using the optimal m-curves, the pressure development as computed by the flow simulator is almost identical to the curve obtained by doing an iterative coupled run. In contrast to Fig. 4, the pressure

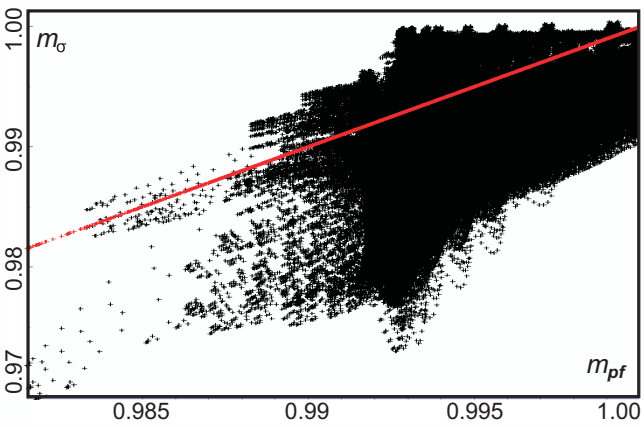

FIGURE 8. Correlation: "exact" m_σ vs. "standard" flow simulator m_{pf}. Coupled run with one iteration (red line: Correlation = 1)

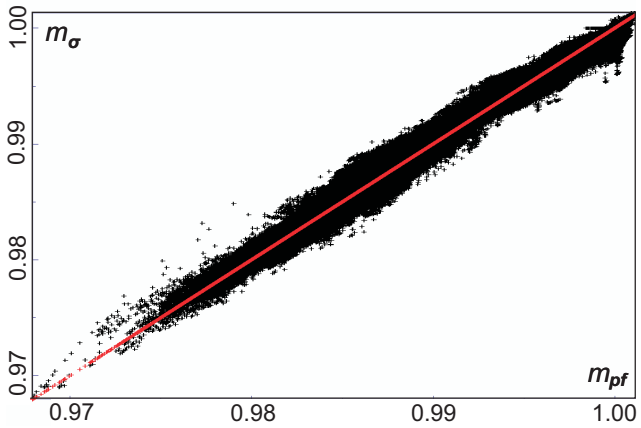

FIGURE 9. Correlation: "exact" m_σ vs. optimal flow simulator m_{pf}. Coupled run with one iteration

from the coupled run is now continuous. The modified m-curves were constructed from six rock mechanics simulations, and the coupled run in this case converged in one iteration, as it should. On the other hand the coupled simulation which was performed to produce Fig. 4 needed 7 iterations to converge, i.e. a total of 42 rock mechanics simulations. Hence by utilizing the modified m-curves CPU-time was reduced to $\approx 1/7$ compared to a standard iterative scheme (which also produced a discontinuous solution).

For larger and more complex models the number of needed iterations in the iterative scheme can easily approach and even exceed 100 for convergence. In practice an upper bound to the number of iterations is therefore often imposed, typically 10–20, but this evidently also influences the quality of the solution. Hence the suggested scheme will often be more accurate than traditional coupled runs in practice, even at the stress steps.

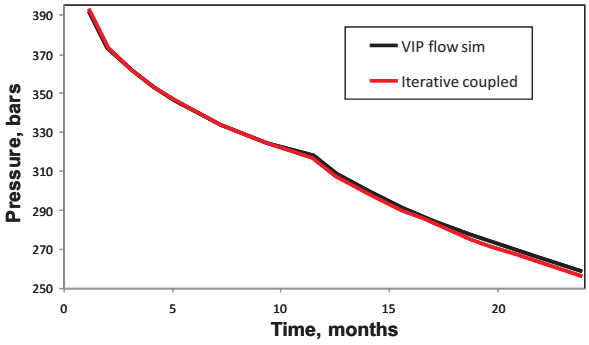

FIGURE 10. Pressure development computed by flow simulator and with iterative coupled simulation, using modified m-curves

8. Conclusions

Rock mechanics effects have significant impact on fluid flow in many reservoirs, and can only be simulated by coupling flow– and rock mechanics equations. The information transfer between these is mainly determined by the cell compaction. A scheme for constructing reliable cell compaction from a few rock mechanics simulations has been presented, based on the concept of pressure-dependent cell pore volume multiplier functions $m_p(p_f, \boldsymbol{x}_i)$, which can be used in further flow simulations. As $m_p(p_f, \boldsymbol{x}_i)$ is the projection of actual cell compaction to p_f-space, it is the best possible approximation to actual pore volume multipliers within the flow equations framework. Hence the flow simulation results will be the best possible achievable. In most cases the approximation is good, and then the stand-alone flow simulator results are reliable as is. Alternatively $m_p(p_f, \boldsymbol{x}_i)$ will act as the optimal initialiser for solving the rock mechanics equations, hence ensuring that the number of needed pore volume iterations is minimised. In practice the obtained results have been found to be at least as accurate as traditional coupled runs, are valid at all times (continuous), and typical computing times have been reduced by some 90–99%.

References

[1] L. Y. Chin, and L. K. Thomas, Fully Coupled Analysis of Improved Oil Recovery by Reservoir Compaction, paper SPE 56753 presented at the SPE Annual Technical Conference and Exhibition, Houston, 3–6. October 1999.

[2] R. H. Dean, X. Gai, C. M. Stone, S. E. Minkoff, A Comparison of Techniques for Coupling Porous Flow and Geomechanics, paper SPE 79709 presented at the SPE Reservoir Simulation Symposium, Houston, 3–5 February, 2003.

[3] M. Gutierrez and R. W. Lewis, The Role of Geomechanics in Reservoir Simulation, paper SPE/IRSM 47392, Proc. Eurock 98 (2) 439–448, Trondheim, Norway, 8–10. July 1998.

[4] M. Gutierrez, R. W. Lewis, I. Masters, Petroleum Reservoir Simulation Coupling Fluid Flow and Geomechanics. SPE Reservoir Engineering & Evaluation 4 (3) (2001), 164–172. SPE 72095-PA.

[5] N. C. Koutsabeloulis, K. J. Heffer, S. Wong, Numerical Geomechanics in Reservoir Engineering. In Computational Methods and Advances in Geomechanics (Ed. Siriwardane & Zeman), 2097–2104, Balkema, Rotterdam, The Netherlands, 1994

[6] N. C. Koutsabeloulis and S. A. Hope, "Coupled" Stress/Fluid/Thermal Multi-Phase Reservoir Simulation Studies Incorporating Rock Mechanics. Paper SPE/IRSM 47393, Proc. Eurock 98, (2) 449–454. Trondheim, Norway, 8–10 July, 1998.

[7] R. W. Lewis, A. Makurat, and W. K. Pao, Fully coupled modeling of seabed subsidence and reservoir compaction of North Sea oil fields, Hydrogeology Journal 11 (2003), 142–161.

[8] P. Longuemare, M. Mainguy, P. Lemonier, A. Onaisi, Ch. Gérard, N. Koutsabeloulis, Geomechanics in Reservoir Simulation: Overview of Coupling Methods and Field Case Study, Oil & Gas Science and Technology – Rev. IFP, 57 (2002), 471–483.
[9] M. Mainguy and P. Longuemare, Coupling Fluid Flow and Rock Mechanics: Formulations of the Partial Coupling between Reservoir and Geomechanical Simulators, Oil & Gas Science and Technology – Rev. IFP, 57 (2002), 355–367.
[10] Ø. Pettersen, Sandstone Compaction, Grain Packing and Critical State Theory, J. Petroleum Geoscience, 13 (2007), 63–67.
[11] Ø. Pettersen and T. G. Kristiansen, Improved Compaction Modeling in Reservoir Simulation and Coupled Rock Mechanics/Flow Simulation, With Examples from the Valhall Field, SPE Reservoir Evaluation & Engineering 12 (2) (2009), 329–340.
[12] Ø. Pettersen, Compaction, Permeability, and Fluid Flow in Brent-Type Reservoirs Under Depletion and Pressure Blowdown, The Open Petroleum Engineering Journal 3 (2010), 1–13
[13] A. Settari and F. M. Mourits, Coupling of geomechanics and reservoir simulation models, In Computational Methods and Advances in Geomechanics (Ed. Siriwardane & Zeman), 2151–2158. Balkema, Rotterdam, The Netherlands, 1994.
[14] A. Settari and F. M. Mourits, A Coupled Reservoir and Geomechanical Modeling System, SPEJ 3 (3) (1998), 219226. SPE 50939-PA.
[15] A. Settari and D. A. Walters, Advances in Coupled Geomechanical and Reservoir Modeling With Applications to Reservoir Compaction, paper SPE 51927 presented at the SPE Reservoir Simulation Symposium, Houston, 14–17 February, 1999.
[16] J. E. Sylte, L. K. Thomas, D. W. Rhett, D. D. Bruning, N. B. Nagel, Water Induced Compaction in the Ekofisk Field, paper SPE 56426 presented at the SPE Annual Technical Conference and Exhibition, Houston, 3–6. October, 1999.
[17] L. K. Thomas, L. Y. Chin, R. G. Pierson, J. E. Sylte, Integrating Geomechanics in Full-Field 3-D Reservoir Simulation – Modeling Techniques and Field Applications, paper SPE 77723 presented at the SPE Applied Technical Workshop, Corpus Christi, Texas, USA 31 July–1 August, 2003
[18] D. M. Wood, Soil Behaviour and Critical State Soil Mechanics, Cambridge University Press, Cambridge, UK, 1990

Centre for Integrated Petroleum Research, Bergen P.O. Box 7810, NO-5020 Bergen, Norway
E-mail: oystein.pettersen@uni.no